Available online at www.sciencedirect.com
SCIENCE DIRECT®
Bioorganic & Medicinal Chemistry Letters 14 (2004) 4505–4509
Bioorganic & Medicinal Chemistry Letters

Isoindolinone ureas: a novel class of KDR kinase inhibitors

Michael L. Curtin,[a,*] Robin R. Frey,[a] H. Robin Heyman,[a] Kathy A. Sarris,[a] Douglas H. Steinman,[a] James H. Holmes,[a] Peter F. Bousquet,[b] George A. Cunha,[b] Maria D. Moskey,[b] Asma A. Ahmed,[b] Lori J. Pease,[a] Keith B. Glaser,[a] Kent D. Stewart,[a] Steven K. Davidsen[a] and Michael R. Michaelides[a]

[a]*Global Pharmaceutical Research and Development, Abbott Laboratories, 100 Abbott Park Road, Abbott Park, IL 60064-6100, USA*
[b]*Global Pharmaceutical Research and Development, Abbott Bioresearch Center, 100 Research Drive, Worcester, MA 01605-5314, USA*

Received 19 May 2004; revised 14 June 2004; accepted 14 June 2004
Available online 6 July 2004

Abstract—A series of substituted isoindolinone ureas was prepared and evaluated for enzymatic and cellular inhibition of KDR kinase activity. Several of these analogs, such as **14c**, are potent inhibitors of KDR both enzymatically (<50 nM) and cellularly (⩽100 nM). A 3D KDR/CDK2/MAP kinase overlay model with several structurally related tyrosine kinase inhibitors was used to predict the binding interactions of the isoindolinone ureas with the KDR active site.

Reversible protein phosphorylation by protein kinases is one of the primary biochemical mechanisms mediating eukaryotic cell signaling.[1] A subset of these kinases, the receptor tyrosine kinases (RTKs), possess both extracellular and intracellular domains and selectively catalyze the phosphorylation of tyrosine hydroxyl groups in response to binding of certain extracellular growth factors.[2] RTK signaling pathways are normally highly regulated, yet their overactivation has been shown to promote the growth, survival, and metastasis of cancer cells and has been associated with the progression of various human cancers.[3] The VEGF receptor family of RTKs, most notably VEGFR2 or KDR, mediates the biological function of vascular endothelial growth factor (VEGF), which is a regulator of vascular permeability and an inducer of endothelial cell proliferation, migration, and survival.[4] Accordingly, interruption of the KDR mediated signaling cascade can provide an anti-angiogenic effect in human cancers as recently demonstrated by the FDA approval of the anti-VEGF antibody Avastin™ for the treatment of colorectal cancer.[5] In addition, several small-molecule KDR kinase inhibitors have been shown to be efficacious in in vivo tumor xenograft models and have entered cancer clinical trials.[6]

In an ongoing effort at Abbott Laboratories to develop small-molecule RTK inhibitors, it was recently disclosed[7] that the diphenyl urea of LCK kinase inhibitor pyrazolopyrimidine **1a** greatly enhanced KDR potency (KDR $IC_{50} = 263$ nM)[8] versus related analogs such as phenyl amide **1b** (KDR IC_{50} >50 μM). This is consistent with earlier observations[9] that variously substituted bis-aryl ureas were potent against a number of protein kinases including p38 MAP, RAF-1, and the CDKs. In an effort to design novel inhibitors of KDR, we believed that the adenine-like pyrrolopyrimidine nucleus of **1** could be replaced with other polycyclic, aromatic systems, which would be capable of making several key hydrogen bond interactions, which are common among ATP-competitive kinase inhibitors.[10] One such nucleus is the isoindolinone of the broad spectrum kinase inhibitor staurosporine[11] (**2**, KDR $IC_{50} = 115$ nM[8]) and, more recently, KDR inhibitor CEP-7055[12] (**3**, KDR $IC_{50} = 18$ nM[13]).[14] Initial modeling of the various regioisomers of diphenyl urea-substituted isoindolinone with KDR indicated that regioisomer **4a** (rings labeled for clarity) could be a viable inhibitor; this idea was validated by the fact that **4a** possessed inhibitory

Keywords: KDR kinase; VEGF; Isoindolinone; Urea.
* Corresponding author. Tel.: +1-847-9380463; fax: +1-847-9355165; e-mail: mike.curtin@abbott.com

0960-894X/$ - see front matter © 2004 Elsevier Ltd. All rights reserved.
doi:10.1016/j.bmcl.2004.06.041

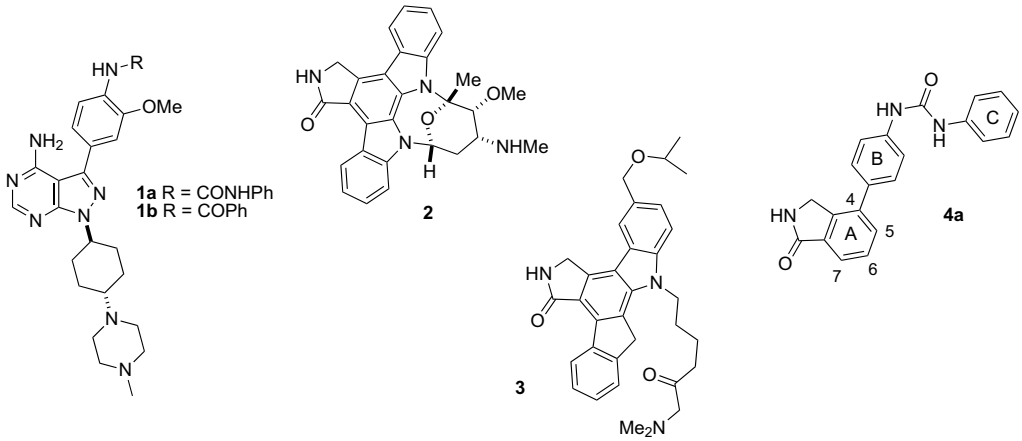

activity, albeit modest, against KDR ($IC_{50} = 1.8\,\mu M$). The synthesis and optimization of this series of KDR inhibitors is reported here.

The straightforward preparation of the isoindolinone ureas began with the esterification and benzylic bromination of 3-bromo-2-methyl benzoic acid to give dibromide **5** (Scheme 1). This intermediate was treated with aq NH_4OH to give lactam **6** in 87% yield. Suzuki coupling gave aniline **7**, which was condensed with variously substituted phenyl isocyanates to afford 4-substituted isoindolinone phenyl ureas **4** in good yields (70–95%).

The syntheses of isoindolinones bearing substituents on the linking phenyl (ring B) began with the preparation of lactam boronate **8** from a palladium catalyzed coupling of bromide **6** with bis(pinacolato)diboron (Scheme 2). Intermediate **8** was coupled with several 2- and 3-substituted 4-bromoanilines to give compounds **9**; these anilines were then converted to diphenyl ureas **10** using the isocyanate method shown in Scheme 1.

Analogs bearing a 7-amino functionality on the isoindolinone (ring A) were made by regioselective nitration of bromolactam **6** with concd HNO_3/H_2SO_4 in excellent yield (Scheme 3). Suzuki coupling of **11** with the 4-boronate of 1-phenyl-(3′-*m*-tolyl) urea gave intermediate **12**, which was reduced to afford amine **13**. Addition to several acid chlorides provided amide analogs **14**.

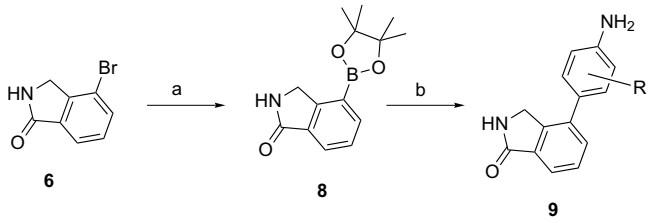

Scheme 2. Reagents and conditions: (a) bis(pinacolato)diboron, cat. $PdCl_2$(dppf), KOAc, DMF, 80 °C, 63%; (b) substituted 4-bromoaniline, cat. $Pd(PPh_3)_4$, Na_2CO_3, DME/H_2O, 90 °C, 50–65%.

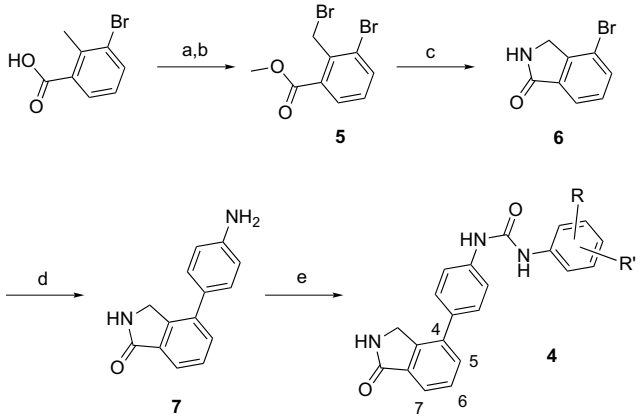

Scheme 1. Reagents and conditions: (a) $SOCl_2$; Et_3N, MeOH, 70%; (b) NBS, cat. Bz_2O_2, PhH, 94%; (c) aq NH_4OH, THF, 87%; (d) 4-(tetramethyldioxaborolanyl)aniline, cat. $Pd(PPh_3)_4$, Na_2CO_3, DME/H_2O, 90 °C, 75%; (e) aryl isocyanate, NMM, THF, 70–95%.

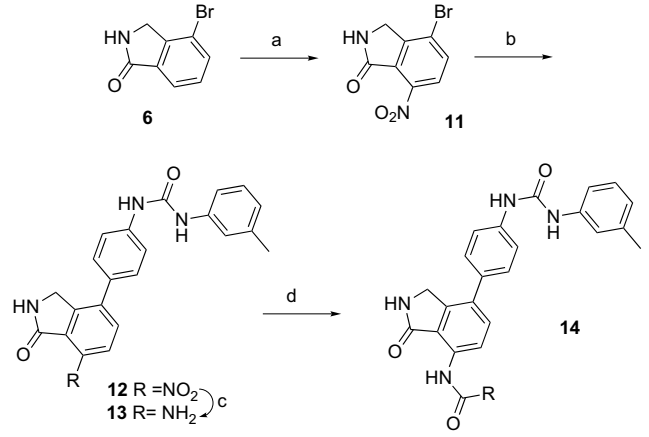

Scheme 3. Reagents and conditions: (a) concd HNO_3, H_2SO_4, 0 °C, 91%; (b) 1-[4-(tetramethyldioxaborolanyl)phenyl]-3′-*m*-tolyl urea, cat. $Pd(PPh_3)_4$, Na_2CO_3, DME/H_2O, 90 °C, 75%; (c) H_2, Pd/C, THF/DMF, 74%; (d) acid chloride, NMM, THF, 70–85%.

Table 1. KDR inhibitory activity of initial isoindolinone analogs

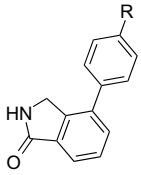

Compds	R	KDR IC_{50} (μM)[8]
4a	–NHCONHPh	1.8
15	–NHCOPh	>50
16	$–NHSO_2Ph$	>50
4b	–NHCONH(3-MePh)	0.1
17	–N(Me)CONH(3-MePh)	1.1
18	–NHCON(Me)(3-MePh)	19
19	$–CH_2CONH$(3-MePh)	2.1
20	$–NHCOCH_2$(3-MePh)	>50
21	–NHC(S)NH(3-MePh)	10

The SAR of the initial isoindolinone compounds is shown in Table 1. Consistent with the KDR inhibitory data for pyrazolopyrimidines **1a**,**b**, the phenyl urea **4a** was much more potent than the phenyl amide (**15**) or sulfonamide (**16**) analogs, which were inactive. The 3-methylphenyl urea (**4b**), which became the baseline urea substitution for this series, showed a significant improvement in activity compared to phenyl urea (**4a**). Methylation of either urea nitrogen (**17**, **18**) gave a significant loss of potency as did replacement with a methylene (**19**, **20**), although the external urea nitrogen (modified in **18** and **20**) appeared to be much more sensitive to these changes. The thiourea **21** also showed a large decrease in activity compared to urea **4b**.

As initial modeling had suggested, the 5-, 6-, and 7-isoindoline urea regioisomers of **4b** (7-regioisomer **22** shown) were inactive against KDR. Replacement of the linking 1,4-phenyl (ring B) with a 1,3-phenyl (**23**, KDR IC_{50} 16 μM) gave a significant loss of potency as did replacement with 2,5-thiophene (compound not shown, KDR IC_{50} 0.7 μM) or pyridyl (**24**, KDR IC_{50} 2 μM). Methylation of the isoindolinone amide nitrogen (**25**, KDR IC_{50} 42 μM) gave nearly a complete loss of inhibitory activity.

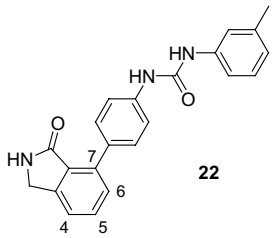

22

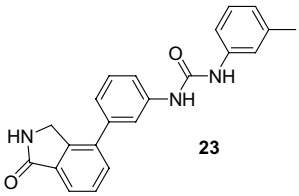

23

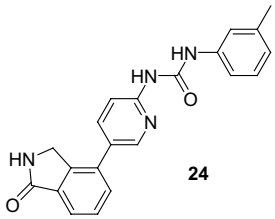

24

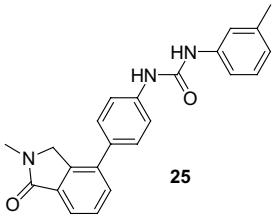

25

Table 2. KDR inhibitory activity of ureas **4**

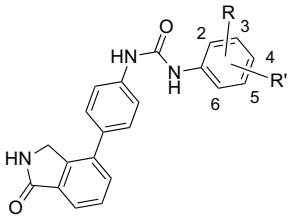

Compds	R	R′	KDR IC_{50} (nM)[8]
4a	H	H	1800
4b	3-Me	H	98
4c	2-Me	H	4400
4d	4-Me	H	430
4e	$3-CF_3$	H	7
4f	$4-CF_3$	H	161
4g	3-Cl	H	46
4h	3-Et	H	29
4i	3-F	H	520
4j	3-OMe	H	570
4k	3-CN	H	370
4l	3-Me	4-Me	50
4m	3-Me	5-Me	83
4n	$3,4-CH_2CH_2CH_2–$		39
4o	$3-CF_3$	6-F	23

The effect of substitution on the terminal urea phenyl (ring C) is shown in Table 2. In general, while most substitution of this phenyl gave improved potency over parent compound **4a**, 3-substitution provided the largest benefit (**4b** vs **4c** or **4d**, **4e** vs **4f**). While several substituents at the 3-position gave potency increases greater than that for 3-methyl (**4e**, **4g**, and **4h**), the benefit of other substituents was modest regardless of their electronic nature or size (**4i**, **4j**, and **4k**). Disubstitution of this phenyl ring (**4l**, **4m**, **4n**, and **4n**) was well tolerated with some substituents.

Substitution of the linking phenyl (ring B) provided a modest improvement in potency as shown in Table 3. Substitution at the 3-position was better tolerated than at the 2-position (**10c** vs **10d**, **10e** vs **10f**) although this

Table 3. KDR inhibitory activity of ureas **10**

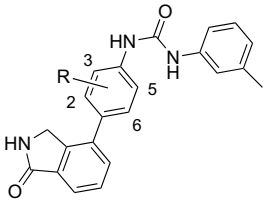

Compds	R	KDR IC_{50} (nM)[8]
10a	2-F	52
10b	3-F	44
10c	2-Me	770
10d	3-Me	19
10e	$2-CF_3$	9000
10f	$3-CF_3$	34
10g	2-Cl	71
10h	3-Cl	30
10i	3-Et	6000
10j	3,5-Me	>50,000

Table 4. KDR inhibitory activity of disubstituted isoindolinones

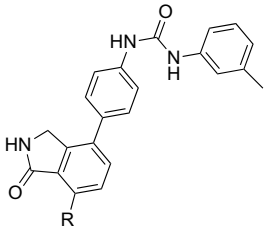

Compds	R	KDR IC_{50} (nM)[8]
13	$–NH_2$	14
14a	–NHAc	64
14b	–NHCOPh	470
14c	–NHCO(3-pyridyl)	10
14d	$–NHCOCH_2NMe_2$	350
26	–OMe	21
27	$–OCH_2CH_2OMe$	126

was not the case for all substituents (**10a** vs **10b**, **10g**, and **10h**). Substitution with groups larger than methyl (**10i**) or disubstitution (**10j**) was not well tolerated.

Table 4 shows the effect on inhibitory potency of substitution at the 7-position of the isoindolinone (ring A). Small substituents such as amino (**13**), acetyl (**14a**), or methoxy (**26**) displayed improved potency versus the parent compound **4b** while larger substituents (**14b**, **14d**, and **27**) were generally not as beneficial, although potent inhibitor **14c** was an exception.

The cellular KDR inhibitory potency of selected compounds is shown in Table 5 and reveals only a modest loss of activity versus the enzymatic data.[15]

The selectivity of analogs **4b** and **14c** for KDR versus other tyrosine kinases as a ratio of enzymatic IC_{50} values is shown in Table 6. These inhibitors had little or no selectivity against the kinases most homologous to KDR (FLT1, FLT4, and KIT) while having much higher selectivity versus TIE2, PDGFRβ, FGFR, and the cytosolic kinase SRC.

A model of inhibitor **4b** bound to the active site of KDR kinase[16] is shown in Figure 1. It was assumed that the lactam of **4b** would occupy the ATP-binding site in an orientation analogous to the corresponding lactam portion of staurosporine (**2**).[17] An overlay model[18] of KDR and CDK2 with bound **2** and **4b** suggested that ATP-mimic hydrogen bonds would be made between the lactam N–H and C=O moieties of **4b** and the KDR protein backbone carbonyl Glu917 and backbone amide Cys919, respectively. This is consistent with the fact that methylation of the lactam nitrogen of **4b** (**25**) led to a complete loss of activity.

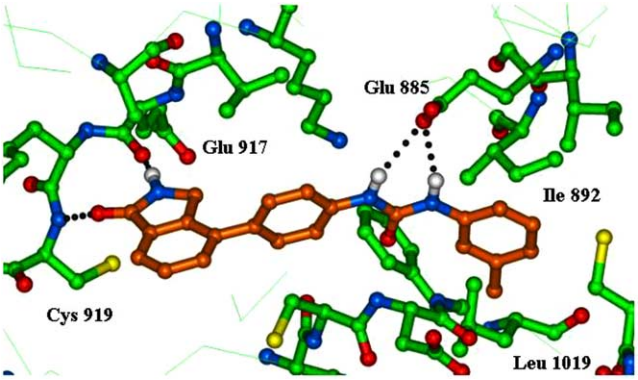

Figure 1. Model of isoindolinone **4b** (brown) bound to the active site of KDR with hydrogen bonds shown as black dotted lines.

A recent crystallographic report disclosed the allosteric binding mode of a diaryl urea (**27**)[19] with p38 MAP kinase that included key hydrogen bond interactions of the urea N–H bonds with Glu71 of that enzyme. Because of the potential binding similarities between ureas **27** and **4b**, the KDR/CDK2/MAP kinase overlay model[18] was used to interrogate the urea–enzyme interactions of **4b** and KDR. As anticipated, this model suggested that the urea of **4b** would make hydrogen bonds to Glu885 of KDR, the residue that corresponds to Glu71 of p38 MAP kinase. These interactions are consistent with the necessity for the urea functionality in the isoindolinone series (**15**, **16**) and the significant loss of potency after urea nitrogen methylation (**17**, **18**) or replacement (**19**, **20**); the apparently more optimal interaction of the 'external' N–H urea bond with Glu885 (3.0 Å vs 3.4 Å for the 'internal' N–H bond as measured in this model) would explain this nitrogen's greater sensitivity to methylation or replacement.

A hydrophobic patch comprised of Ile892 and Leu1019 of KDR appeared to accommodate the tolyl unit of **4b**, although this model could not completely explain the varied effects of other substituents on this ring. Finally, the fact that most substitution was allowed at both the linking phenyl (e.g., **10f**) and the 7-position of the isoindolinone (e.g., **14c**) is consistent with the overlay model, which indicated the presence of unoccupied volume near these positions.

Table 5. Enzymatic and cellular KDR inhibition of selected compounds

Compds	KDR IC_{50} (nM)[8]	Cell IC_{50} (nM)[15]
4b	98	270
4e	7	65
4o	23	150
10d	19	68
10h	30	99
14c	10	11
26	21	170

Table 6. KDR fold-selectivity versus a series of tyrosine kinases

Compds	FLT1	FLT4	KIT	TIE2	PDGFRβ	FGFR	SRC
4b	6.5	0.6	0.1	33	>500	>500	>500
14c	21	0.6	2	1700	>4500	>4500	>4500

In summary, a series of potent KDR isoindolinone inhibitors has been identified. Optimal substitution afforded analogs with significant enzymatic and cellular potency as well as selectivity against several non-VEGF tyrosine kinases. A 3D kinase overlay model suggested that the predominant isoindolinone/KDR interactions include hydrogen-bonds between the inhibitor lactam moiety and the protein backbone as well as the urea functionality and a glutamate residue.

References and notes

1. Hunter, T. *Cell* **2000**, *100*, 113–127.
2. (a) Manning, G.; Whyte, D. B.; Martinez, R.; Hunter, T.; Sudarsanam, S. *Science* **2002**, *298*, 1912–1934; (b) Robinson, D. R.; Wu, Y. M.; Lin, S. F. *Oncogene* **2000**, *19*, 5548–5557.
3. Blume-Jensen, P.; Hunter, T. *Nature* **2001**, *411*, 355–365.
4. Ferrara, N.; Gerber, H. P.; LeCouter J. *Nat. Med.* **2003**, *9*, 669–676.
5. Dvorak, H. F. *J. Clin. Oncol.* **2002**, *20*, 4368–4380.
6. For a recent review see: Manley, P. W.; Bold, G.; Bruggen, J.; Fendrich, G.; Furet, P.; Mestan, J.; Schnell, C.; Stolz, B.; Meyer, T.; Meyhack, B.; Stark, W.; Strauss, A.; Wood, J. *Biochim. Biophys. Acta* **2004**, *1697*, 17–27.
7. Burchat, A. F.; Calderwood, D. J.; Friedman, M. M.; Hirst, G. C.; Li, B.; Rafferty, P.; Ritter, K.; Skinner, B. S. *Bioorg. Med. Chem. Lett.* **2002**, *12*, 1687–1690.
8. KDR IC_{50} values were determined by an assay of nonphosphorylated KDR active kinase domain (soluble *C*-terminal domain with a *N*-terminal 6-His sequence to facilitate purification, cloned, and expressed in baculovirus) using an ATP concentration of 1 mM. A biotinylated peptide substrate containing a single tyrosine was used in a microtiter plate assay using HTRF® methodology as described in Kolb, A. J.; Kaplita, P. V.; Hayes, D. J.; Park, Y.-W.; Pernell, C.; Major, J. S.; Mathias, G. *Drug Discov. Today* **1998**, *3*, 333–342. Inhibition constants are the mean of two determinations performed with seven concentrations of the test compounds.
9. Dumas, J. *Curr. Opin. Drug Discov. Dev.* **2002**, *5*, 718–727.
10. Toledo, L. M.; Lydon, N. B.; Elbaum, D. *Curr. Med. Chem.* **1999**, *6*, 775–805.
11. Tamaoki, T.; Nomoto, H.; Takahashi, I.; Kato, Y.; Morimoto, M.; Tomita, F. *Biochem. Biophys. Res. Commun.* **1986**, *135*, 397–402.
12. Gingrich, D. E.; Reddy, D. R.; Iqbal, M. A.; Singh, J.; Aimone, L. D.; Angeles, T. S.; Albom, M.; Yang, S.; Ator, M. A.; Meyer, S. L.; Robinson, C.; Ruggeri, B. A.; Dionne, C. A.; Vaught, J. L.; Mallamo, J. P.; Hudkins, R. L. *J. Med. Chem.* **2003**, *46*, 5375–5388.
13. The given IC_{50} was taken from Ref. 12 and was run using an ATP concentration of 16 μM.
14. For an earlier synthetic report of related isoindolinones, see: Rupert, K. C.; Dodd, J. H.; Henry, J. R. *Heterocycles* **1997**, *45*, 2217–2221.
15. The cellular IC_{50} values represent inhibition of KDR phosphorylation in NIH3T3 cells stably transfected with full length human KDR. Cells were stimulated with human recombinant VEGF (50 ng/mL) for 10 min in the presence of compound, after which the cells were lysed and phosphorylated KDR determined by ELISA. KDR ELISA consisted of an anti-KDR (R&D Systems) capture antibody and anti-phosphotyrosine (4G10, UBI) horseradish peroxidase-conjugated detection antibody. Inhibition of VEGF induced phosphorylation was determined relative to a nonphosphorylated control, and IC_{50} values calculated by nonlinear regression analysis of the concentration–response curve. Each IC_{50} determination was preformed with five concentrations and each assay point determined in duplicate.
16. The model was constructed by using the published crystal structure of unliganded KDR enzyme (PDB entry 1VR2) in: McTigue, M. A.; Wickersham, J. A.; Pinko, C.; Showalter, R. E.; Parast, C. V.; Tempczyk-Russell, A.; Gehring, M. R.; Mroczkowski, B.; Kan, C.-C.; Villafranca, J. E.; Appelt, K. *Structure* **1999**, *7*, 319–330. This structure corresponds to KDR with a doubly-phosphorylated activation loop in a closed conformation, but with much of the loop disordered and presumed to be conformationally mobile. The modeling studies reported here focused on regions of the protein that were crystallographically well defined. No modifications to the protein structure were made to account for the flexible activation loop.
17. The crystallographically observed orientation of **2** in CDK2 kinase (PDB entry 1AQ1) was used as a source of the staurosporine orientation.
18. A 3D overlay of kinase crystal structures of KDR, CDK2, and p38 MAP kinases was created by selecting 12 spatially equivalent residues from each of the three active sites. Six of these residues were derived from the hinge region and six were from the other regions of the active site. A least-squares superposition of the alpha carbons from these 12 residues provided a reasonable active site overlay. The 12 residues for each enzyme are listed as follows: KDR (PDB 1VR2) Ala866, Lys868, Val914, Ile915, Val916, Glu917, Phe918, Cys919, Asn1033, Leu1035, Cys1045, and Asp1046; CDK2 (PDB 1AQ1) Ala31, Lys33, Leu78, Val79, Phe80, Glu81, Phe82, Leu83, Asn132, Leu134, Ala144, and Asp145; p38 MAP (PDB 1KV1) Ala51, Lys53, Leu104, Val105, Thr106, His107, Leu108, Met109, Asn155, Ala157, Leu167, Asp168.
19. For the crystal structure of urea **27** bound to p38 MAP kinase (PDB entry 1KV1), see: Pargellis, C.; Tong, L.; Churchill, L.; Cirillo, P. F.; Gilmore, T.; Graham, A. G.; Grob, P. M.; Hickey, E. R.; Moss, N.; Pav, S.; Regan, J. *Nature Struct. Biol.* **2002**, *9*, 268–272.

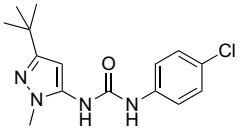

27